

Performance assessment of advanced hollow RC bridge column sections

T.H. Kim¹, H.Y. Kim², S.H. Lee¹, J.H. Lee² and H.M. Shin^{*3}

¹Technology Development Team, Samsung Construction & Trading Corporation,
5th Fl., Daerung Gangnam Tower, 826-20 Yeoksam1-dong, Gangnam-gu, Seoul 135-935, Korea

²Department of Civil Engineering, Yeungnam University, 214-1 Dae-dong, Gyeongsan-si,
Gyeongsangbuk-do, 712-749, Korea

³School of Civil and Architectural Engineering, Sungkyunkwan University, 300 Cheoncheon-dong,
Jangan-gu, Suwon-si, Gyeonggi-do, 440-746, Korea

(Received June 12, 2015, Revised October 27, 2015, Accepted October 30, 2015)

Abstract. This study investigates the performance of advanced hollow reinforced concrete (RC) bridge column sections with triangular reinforcement details. Hollow column sections are based on economic considerations of cost savings associated with reduced material and design moments, as against increased construction complexity, and hence increased labor costs. The proposed innovative reinforcement details are economically feasible and rational, and facilitate shorter construction periods. We tested a model of advanced hollow column sections under quasi-static monotonic loading. The results showed that the proposed triangular reinforcement details were equal to the existing reinforcement details, in terms of the required performance. We used a computer program, Reinforced Concrete Analysis in Higher Evaluation System Technology (RCAHEST), for analysis of the RC structures; and adopted a modified lateral confining effect model for the advanced hollow bridge column sections. Our study documents the testing of hollow RC bridge column sections with innovative reinforcement details, and presents conclusions based on the experimental and analytical findings. Additional full-scale experimental research is needed to refine and confirm the design details, especially for the actual detailing employed in the field.

Keywords: performance; hollow; column sections; triangular reinforcement details; cost savings; construction periods

1. Introduction

Hollow bridge column sections are used because they offer the advantages of high bending and torsional stiffness, reduced substructure weight, and consequent savings in foundation costs Han *et al.* (2014), Kim *et al.* (2013), Lignola (2006), Yukawa *et al.* (1999). For these reasons, RC bridge columns with hollow sections are widely designed and constructed for highway, high-speed rail, and other bridge columns.

However, modern codes AASHTO (2012), Eurocode (2004), MCT (2010) of practice oriented

*Corresponding author, Professor, E-mail: hmshin@skku.edu

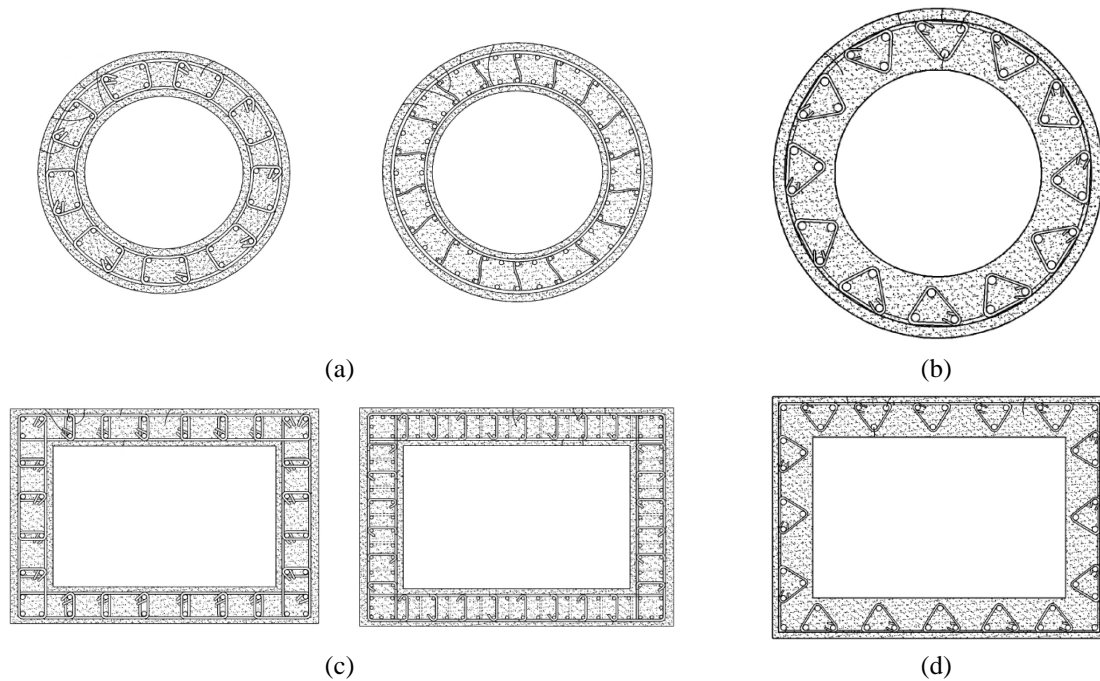


Fig. 1 Hollow RC bridge column sections with reinforcement details for material quantity reduction Kim *et al.* (2013): (a) existing reinforcement details (circular sections), (b) proposed reinforcement details (circular sections), (c) existing reinforcement details (rectangular sections) and (d) proposed reinforcement details (rectangular sections)

to new design do not recognize any specific problem related to hollow sections, probably because of a lack of knowledge Delgado *et al.* (2008), Kim *et al.* (2013), Papanikolaou and Kappos (2009) Yeh *et al.* (2002).

Hollow bridge column sections are based on economic considerations of the cost saving associated with reduced material and design moments, as against the increased construction complexity, and hence increased labor costs.

The objectives of our study were to experimentally and analytically investigate the performance of advanced hollow RC bridge column sections with triangular reinforcement details. We expected the proposed innovative reinforcement details to exhibit sufficient ductility and design strength, and intended them to provide a baseline result for comparison with existing reinforcement details.

We performed a series of tests, in which ten hollow column section specimens were loaded to failure under pure axial load. Many parameters may influence the overall hollow section response, such as the reinforcement details, the shape of the section, the spacing of the transverse reinforcement, and finally, the material strength of the concrete and reinforcement.

We propose an evaluation method for the performance of advanced hollow RC bridge column sections with triangular reinforcement details. The proposed method uses a nonlinear finite element analysis program, RCAHEST, which was developed by the authors Kim *et al.* (2002, 2003, 2007, 2009, 2013, 2014). We adopted a modified lateral confining effect model for advanced hollow bridge column sections. We implemented this model in a computer program called RCAHEST, and conducted a parameter study.

Table 1 Properties of test specimens

Specimen	Strength of concrete (MPa)	Longitudinal reinforcement		Transverse reinforcement		
		Yield strength (MPa)	Ratio	Yield strength (MPa)	Volumetric Ratio (Compared to MCT code)	
C-RHC-BS	29.2	488	0.013	511	0.0058 (80%)	
C-RHT-BS			0.012		0.0077 (107%)	
C-RHT-IT*					0.0077 (107%)	
C-RHT-BD					0.0039 (54%)	
C-RHT-BN					0.0019 (27%)	
C-CHC-BS	25.8	536	0.016	482	0.0031 (43%)	
C-CHT-BS	25.8				0.0031 (43%)	
C-CHT-IT*	31.3				0.0031 (43%)	
C-CHT-BD	30.1				0.0016 (22%)	
C-CHT-BN	31.3				0.0010 (14%)	

Note: * Only outer lateral reinforcement

Our paper presents simulations performed in large-scale experiments on advanced hollow RC bridge column sections with triangular reinforcement details. On the basis of the experimental observations and analytical modeling, we developed design guidelines for hollow RC bridge column sections with reinforcement details for material quantity reduction.

2. Advanced hollow RC bridge column sections with triangular reinforcement details

Fig. 1 shows the developed hollow RC bridge column sections with reinforcement details for material quantity reduction Kim *et al.* (2013).

In existing practice, a number of layers of longitudinal and transverse steel are placed near both the outside and inside faces of hollow circular section for bridge columns, and are tied through the wall thickness with cross-ties. Normally, a 135-degree bend or full hook should be specified for at least one end of the cross-tie. These hollow column sections have increased construction complexity, and hence increased labor costs.

In previous study Kim *et al.* (2013), developed reinforcement details for material quantity reduction consist of a stable triangular structure that combines outside transverse reinforcement and triangular cross-ties with satisfactory reduction, inside transverse reinforcement. The transverse steel placed near the inside face and the cross-ties may not significantly contribute to the confinement of the concrete wall in the hollow section Hoshikuma *et al.* (2000), Zahn *et al.* (1990). The details involve applying a sparsely spaced inner reinforcement in circular hollow sections, in order to control cracking due to environmental effects (the serviceability limit state).

This paper presents a new design concept of advanced hollow RC bridge column sections with reinforcement details for material quantity reduction. Our proposed innovative reinforcement

details offer economic feasibility and rationality, and facilitate shorter construction periods. This will ensure a proper understanding of structural behavior, and thus help develop a conservative approach for analysis and design.

3. Experimental investigation

3.1 Test specimens and test procedure

Table 1 lists the mechanical properties of the specimens, and Figs. 2 and 3 show the geometric details.

The experimental program consisted of compression tests to failure of ten hollow column section specimens. The size of specimens was determined according to the capacity of a testing

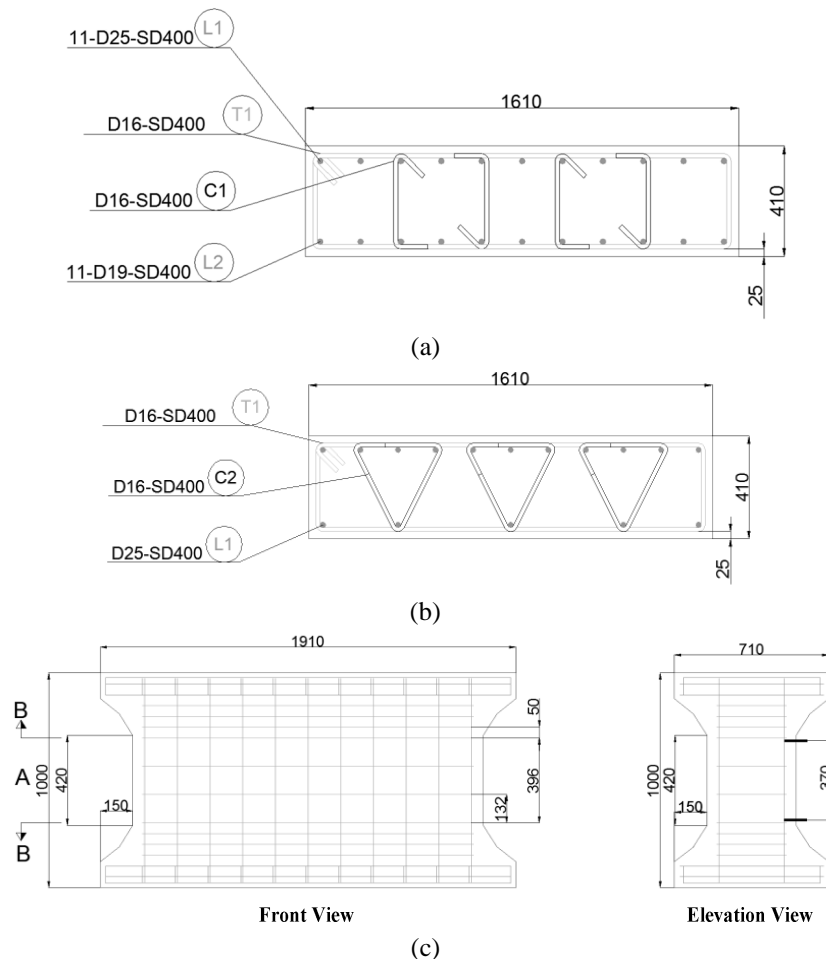


Fig. 2 Rectangular test specimens (Unit: mm): (a) section view (existing details); (b) section view (developed details); (c) specimens C-RHC-BS / C-RHT-BS / C-RHT-IT; (d) specimen C-RHT-BD; and (e) specimen C-RHT-BN

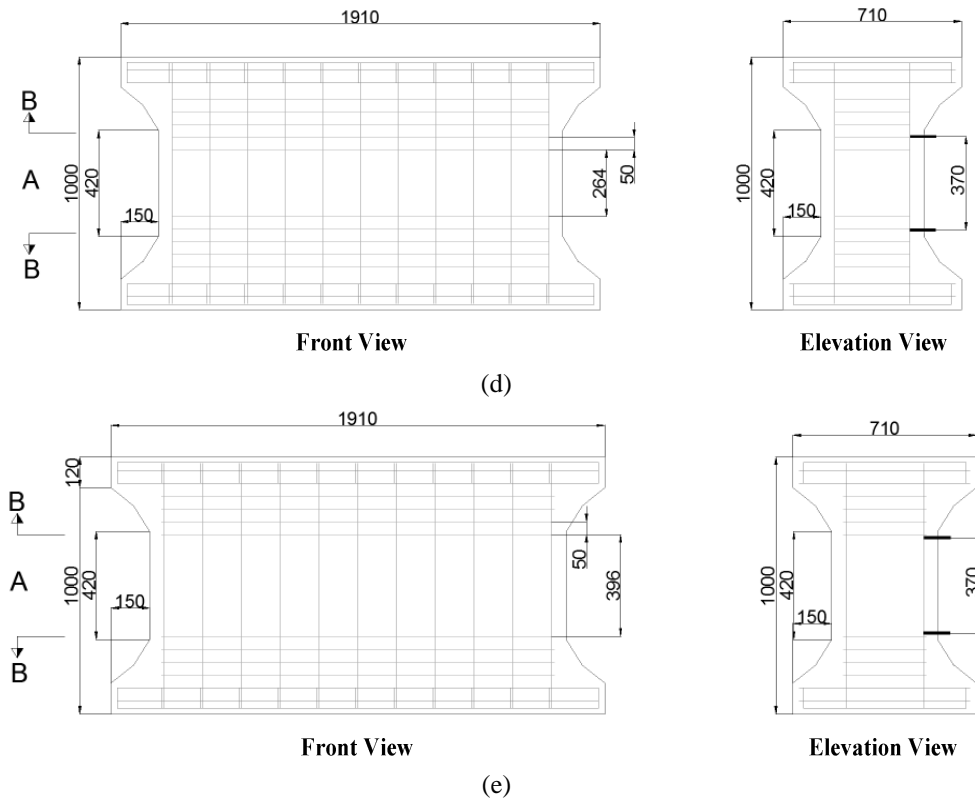


Fig. 2 Continued

machine. We loaded the specimens to induce central axial compression. Solid, heavily reinforced load heads, cast integrally with each specimen, distributed the load from the test machine to the hollow cross section.

We designed four rectangular specimens with innovative reinforcement details for testing under monotonic loading, designated as C-RHT-BS, C-RHT-IT, C-RHT-BD and C-RHT-BN. In addition, we designed one specimen for existing reinforcement details under monotonic loading, designated as C-RHC-BS (see Figs. 2(a) and (c)). The height-to-width ratio for all specimens was 0.6. The reinforcement volumetric ratio of C-RHT-BS to C-RHC-BS equals 1.0.

In addition, we designed four circular specimens with innovative reinforcement details for testing under monotonic loading, designated as C-CHT-BS, C-CHT-IT, C-CHT-BD and C-CHT-BN. In addition, we designed one specimen for the existing reinforcement details under monotonic loading, designated as C-CHC-BS (see Figs. 3(a) and (c)). The height-to-width ratio was 0.5.

The first character of the specimen name refers to the element level specimen (C); the second character stands for the shape of the section (Circular or Rectangular); the third character represents the hollow column section (H); the fourth character refers to the configuration type (C or T); and the fifth and sixth characters taken together represent the reinforcement details (BS, IT, BD, or BN).

BS or IT represents six times the diameter of the longitudinal reinforcement. BD represents twelve times the diameter of the longitudinal reinforcement. BN represents only triangular cross-

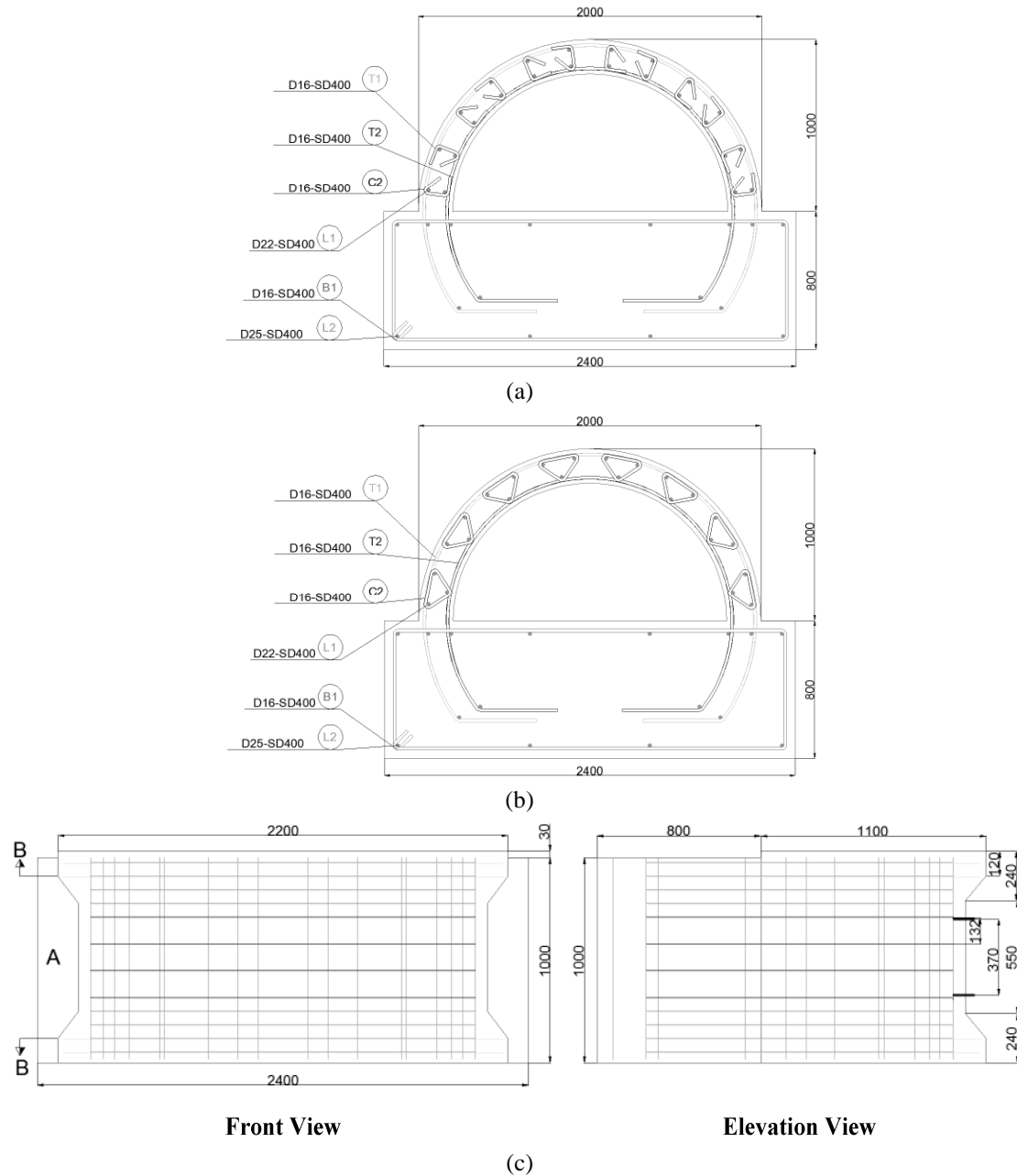


Fig. 3 Circular test specimens (Unit: mm): (a) section view (existing details); (b) section view (developed details); (c) specimens C-CHC-BS / C-CHT-BS / C-CHT-IT; (d) specimen C-CHT-BD; and (e) specimen C-CHT-BN

ties, since the aim of our study is also to investigate the behavior of advanced hollow cross sections. In this paper, the spacing of the confining steel conservatively satisfies the requirement specified in the MCT Code (2010).

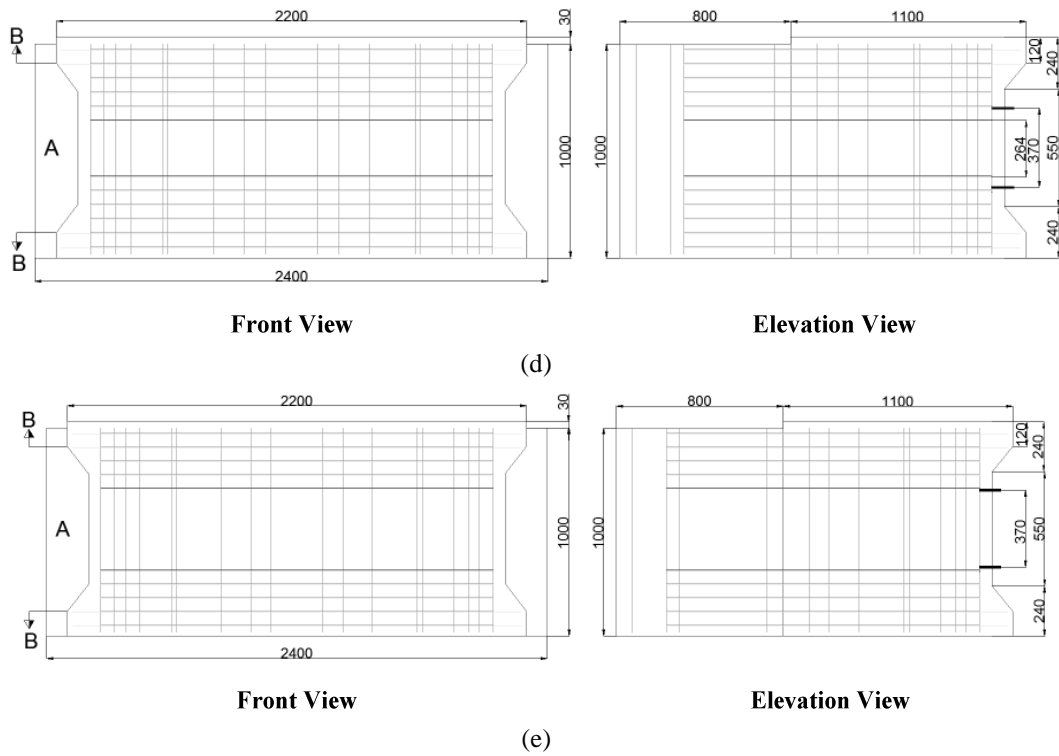


Fig. 3 Continued

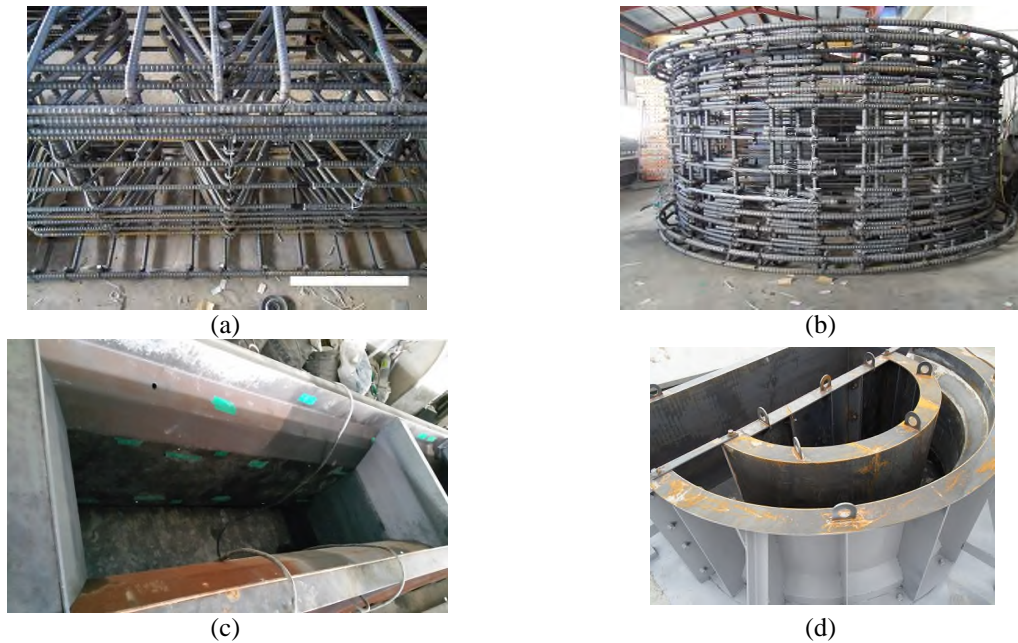


Fig. 4 Construction sequence: (a) reinforcement cage for rectangular sections; (b) reinforcement cage for circular sections; (c) mold for rectangular sections; (d) mold for circular sections; (e) rectangular specimen after casting; and (f) circular specimen after casting



Fig. 4 Continued



Fig. 5 Loading setup

The specimens were tested using a testing machine with a capacity of 30 MN (see Fig. 5). Thick steel plates were attached to the top and bottom of each specimen.

The axial force was monotonically increased at 0.01 mm/sec, until the maximum force of the specimen was reached.

3.2 Results of experiments

Figs. 6 and 7 show the axial load-versus-axial strain relationships for specimens, which also show the design axial strength of the column section, and the damage pattern of the specimens at failure. The design axial strengths obtained from the design code MCT (2010) are conservative, both for specimens with innovative and existing reinforcement details.

These figures indicate that the damage to the specimen was spalling of the outer layer of the concrete cover. We observed a few longitudinal bars buckled outward between the layers of lateral reinforcement after failure. Such buckling of longitudinal bars is to be expected, since the concrete

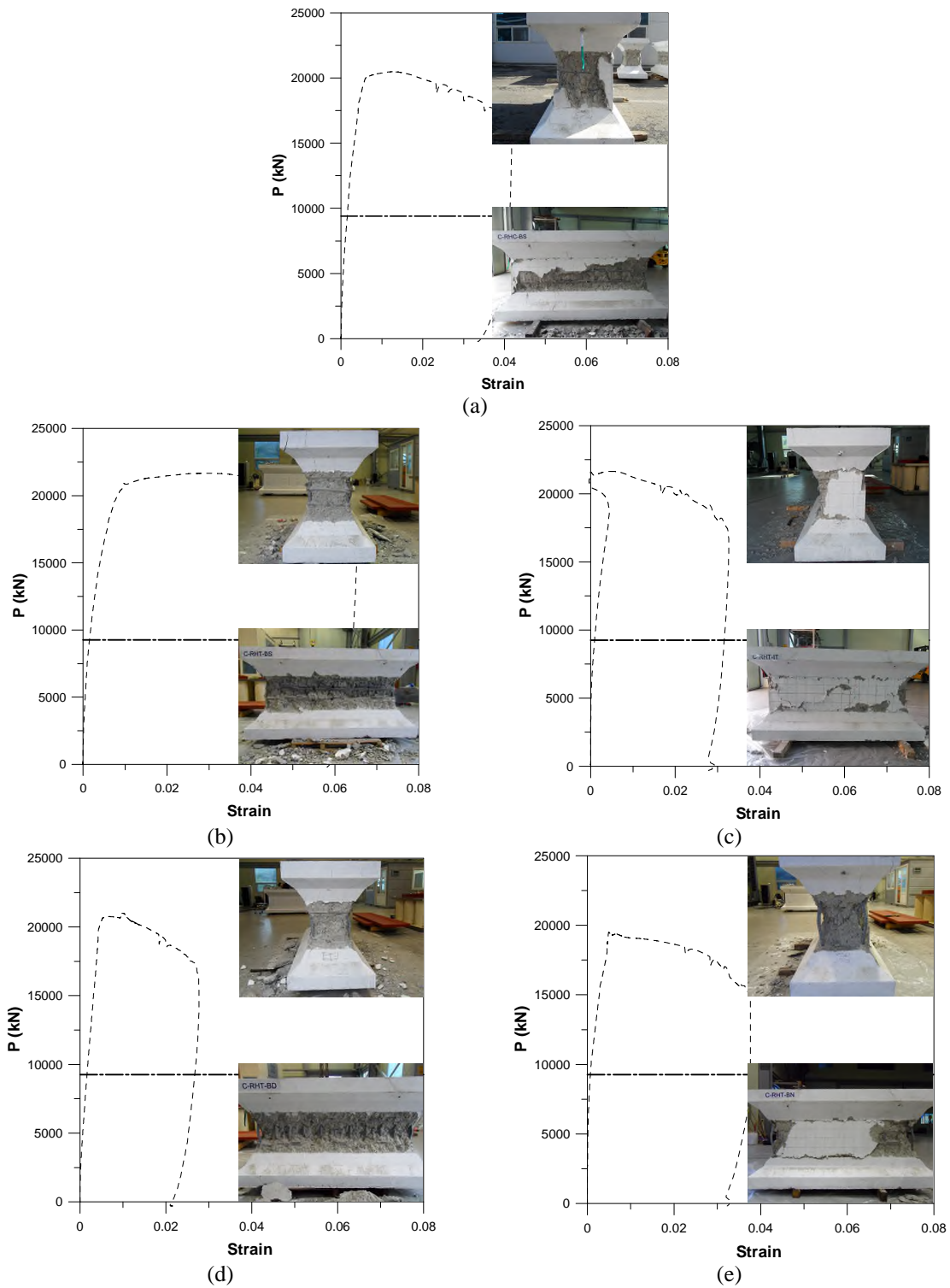


Fig. 6 Axial Load-versus-axial strain relationship: (a) specimen C-RHC-BS; (b) specimen C-RHT-BS; (c) specimen C-RHT-IT; (d) specimen C-RHT-BD; and (e) specimen C-RHT-BN

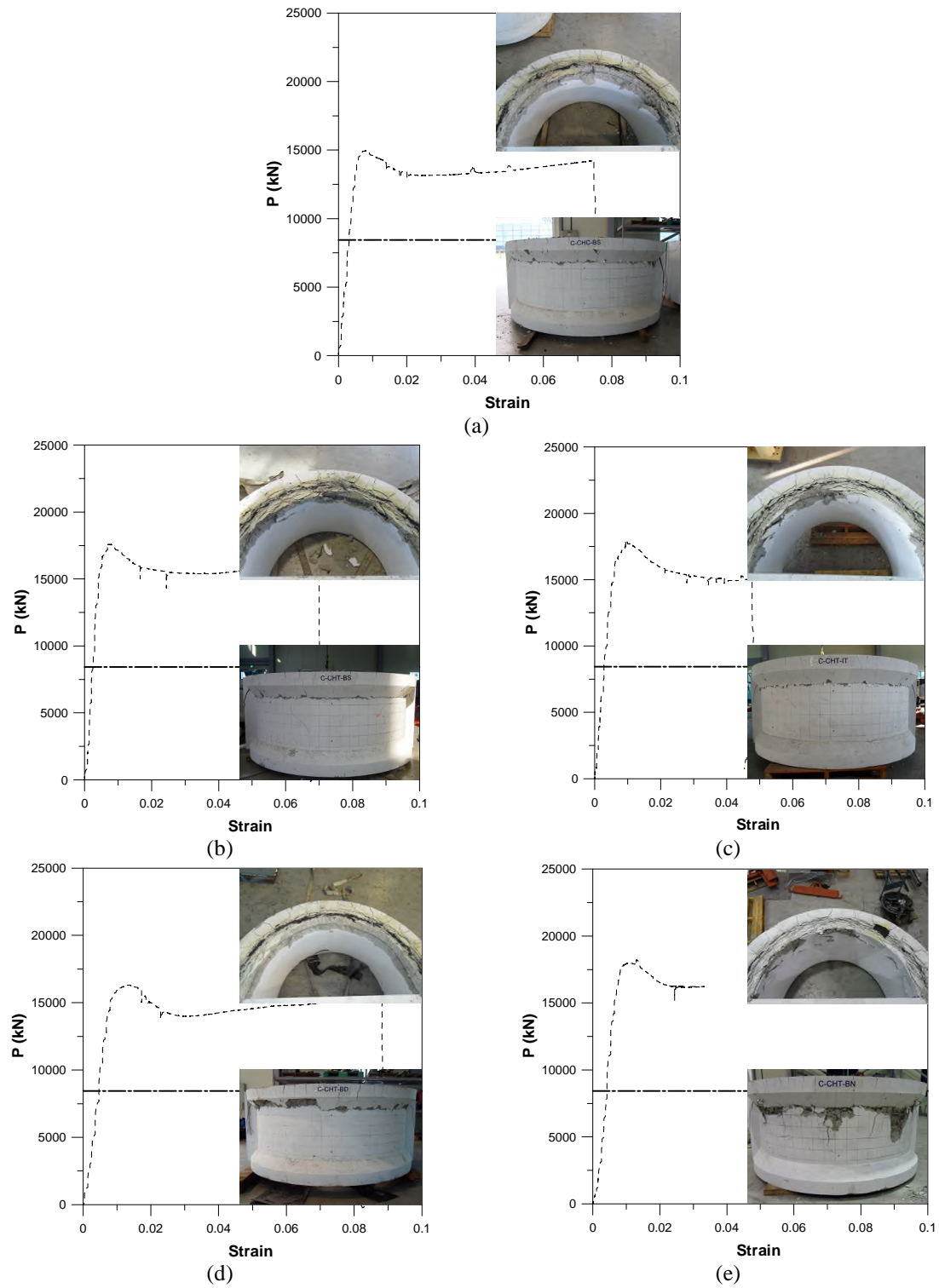


Fig. 7 Axial Load-versus-axial strain relationship: (a) specimen C-CHC-BS; (b) specimen C-CHT-BS; (c) specimen C-CHT-IT; (d) specimen C-CHT-BD; and (e) specimen C-CHT-BN

Table 2 Experimental results

Specimen	ϕP_n (kN)	P_n (kN)	P_{cr} (kN)	P_{max} (kN)	$\frac{P_{max}}{\phi P_n}$	$\frac{P_{max}}{P_n}$	$\varepsilon_{P_{cr}}$	$\varepsilon_{P_{max}}$	$\varepsilon_{0.85 P_{max}}$
C-RHC-BS	9395.7	16778.1	7000.0	20475.3	2.18	1.22	0.0009	0.0123	0.0388
C-RHT-BS	9264.4	16543.5	5000.0	21668.7	2.34	1.31	0.0005	0.0288	0.0583
C-RHT-IT	9264.4	16543.5	5000.0	21647.5	2.34	1.31	0.0001	0.0050	0.0293
C-RHT-BD	9264.4	16543.5	4500.0	21004.1	2.27	1.27	0.0005	0.0101	0.0249
C-RHT-BN	9264.4	16543.5	7000.0	19512.4	2.11	1.18	0.0003	0.0050	0.0326
C-CHC-BS	8435.1	15062.6	7800.0	14946.0	1.77	0.99	0.0027	0.0079	0.0183
C-CHT-BS	8435.1	15062.6	6000.0	17638.8	2.09	1.17	0.0020	0.0069	0.0244
C-CHT-IT	8435.1	15062.6	4500.0	17930.2	2.13	1.19	0.0015	0.0094	0.0278
C-CHT-BD	8435.1	15062.6	7000.0	16303.7	1.93	1.08	0.0038	0.0140	0.0229
C-CHT-BN	8435.1	15062.6	6000.0	18223.6	2.16	1.21	0.0033	0.0130	0.0244

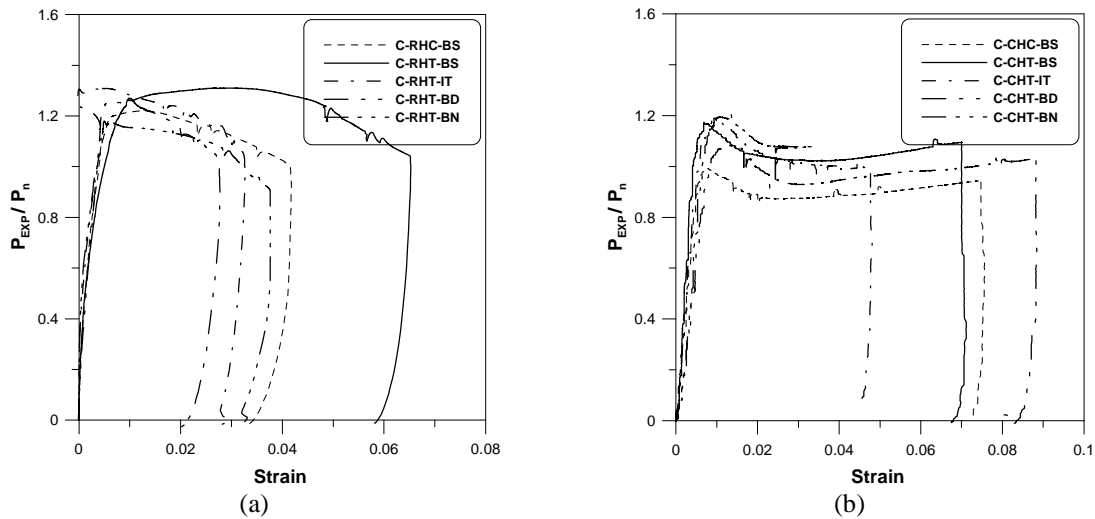


Fig. 8 Normalized load-versus-axial strain relationship for specimens: (a) rectangular series; and (b) circular series

that surrounds and supports the bars is suddenly lost in an explosive failure. After the maximum state, we observed the buckling of reinforcement and spalling of concrete, and the restoring force decreased rapidly. We observed two failure modes: concrete crushing and reinforcing bar buckling.

Table 2 presents the total design axial strength (ϕP_n), nominal axial strength (P_n) and maximum axial load (P_{max}) of test specimens. This table shows the strain, $\varepsilon_{P_{max}}$ corresponding to peak load and on the softening branch at 85 percent of ultimate load, $\varepsilon_{0.85 P_{max}}$ Eurocode (2004). Table 2 also shows that specimens with the proposed innovative reinforcement details showed sufficient ductility prior to the abrupt failure.

Fig. 8 shows the normalized axial load-versus-axial strain relationships for rectangular specimens and circular specimens. As a result, the required performance of the triangular

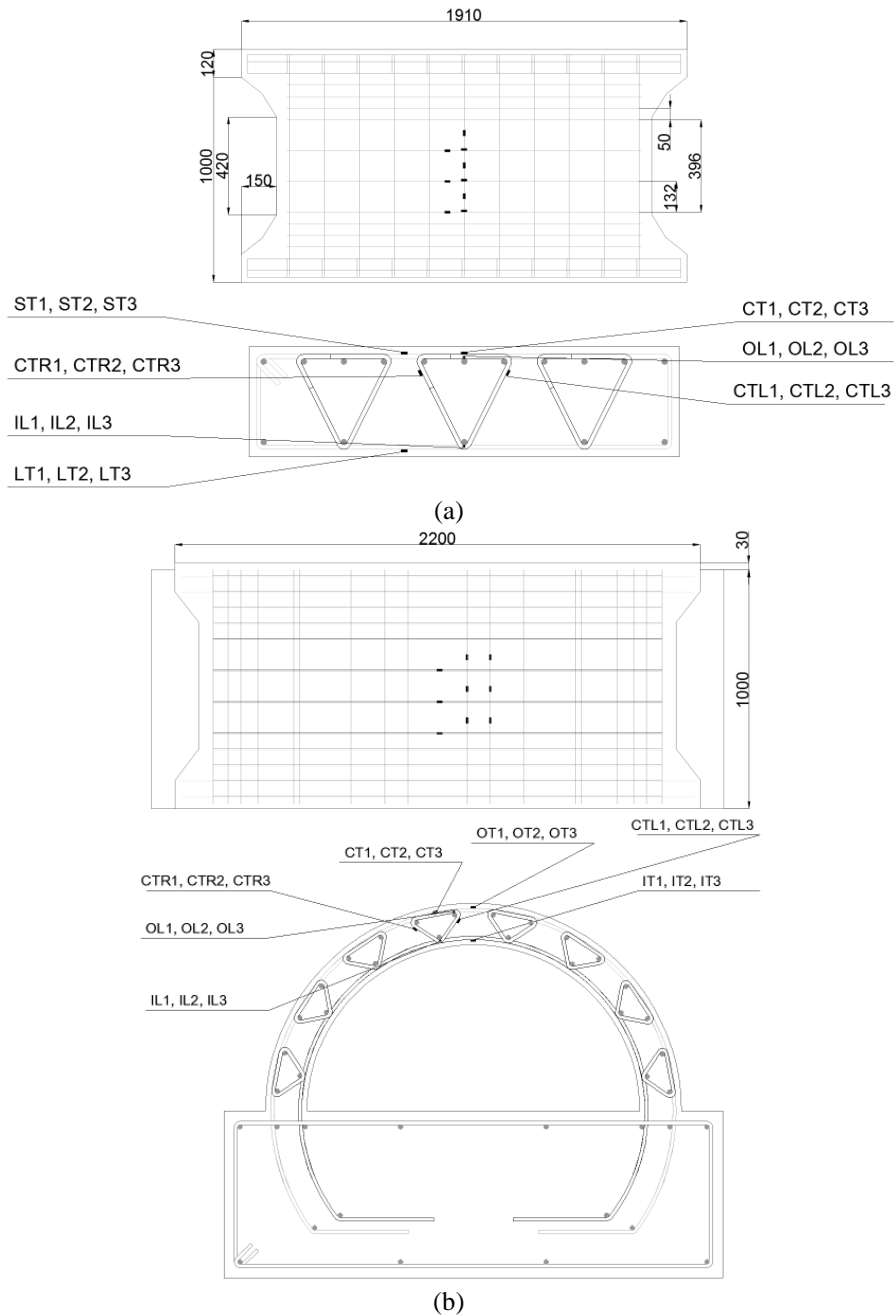


Fig. 9 Instrumentation of the test specimen (Unit: mm): (a) rectangular section; and (b) circular section

reinforcement details was the same as those for the existing reinforcement details.

Instrumentation included measurements of load, reinforcement strains, and displacements, including the displaced shape of the compression face of the section (see Fig. 5). Strain in the longitudinal and transverse reinforcement was measured by the strain gages attached at the

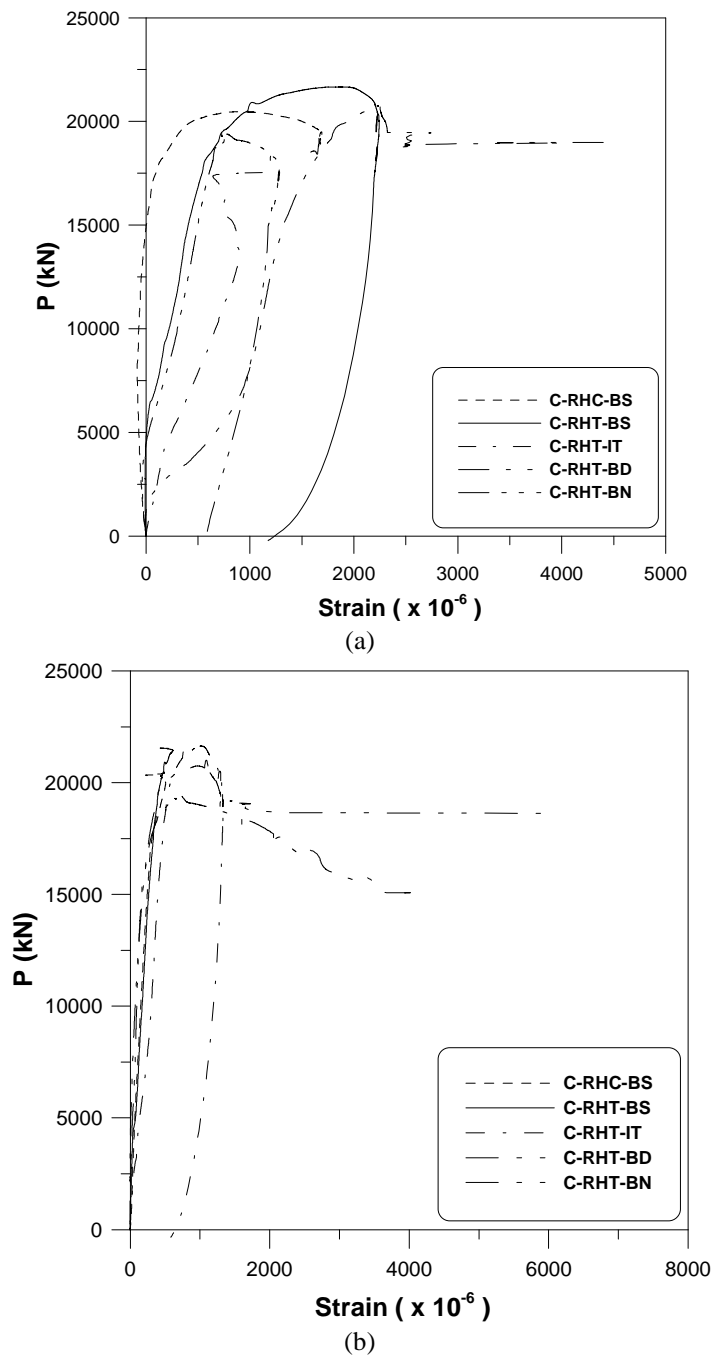


Fig. 10 Axial load-strain curves of transverse reinforcement for rectangular specimens: (a) ST; and (b) CTR

positions shown in Fig. 9. Strains in reinforcing bars were measured using electric resistance strain gages.

Figs. 10 and 11 show the typical measured steel strains in the transverse reinforcement for

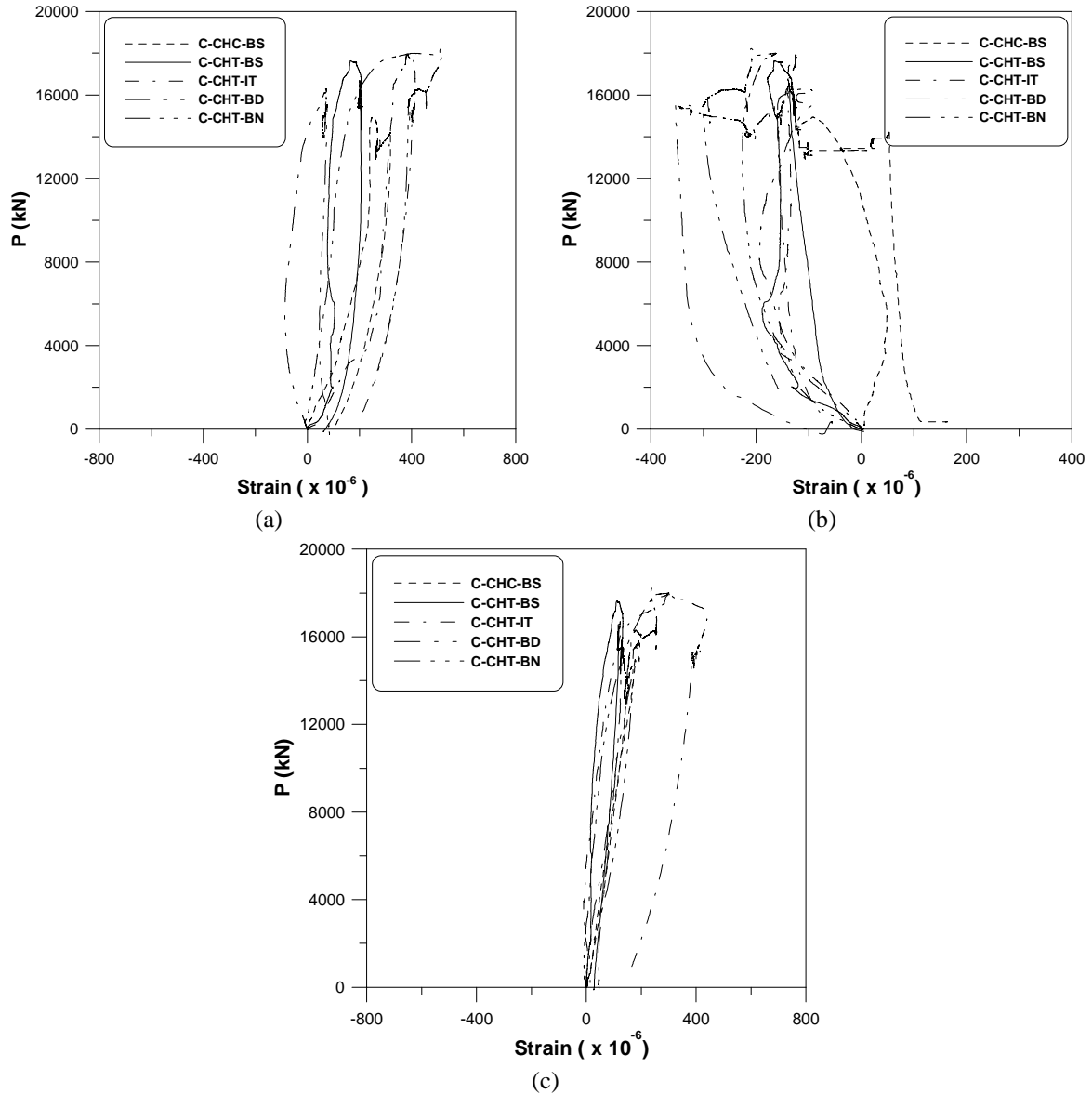


Fig. 11 Axial load-strain curves of transverse reinforcement for circular specimens: (a) OT; (b) IT; and (c) CTR

specimens. In most cases, the specimen showed maximum strain in the transverse reinforcements lower than the yield strain. Some steel strains appear to have reached 6000 microstrain. Fig. 11(b) shows that the effect of negative confinement (cracking of the inner concrete cover) diminishes, because the links' tensile actions transfer the confining action of the inner transverse reinforcement towards the outer transverse reinforcement, providing improved confinement of the concrete region in-between. We also observed that the presence of an inner transverse reinforcement does not significantly contribute to the strength and ductility of the confined section.

4. Analytical investigation

4.1 Numerical simulation

We developed a two- and three-dimensional finite element model for the advanced hollow RC bridge column sections with triangular reinforcement details in this study. We created and analysed the model using general-purpose finite element software, RCAHEST Kim *et al.* (2002, 2003, 2007, 2009, 2013, 2014). RCAHEST is a nonlinear finite element analysis program that is used for analysing RC structures (see Fig. 12).

The proposed structural element library RCAHEST is built around the finite element analysis program shell named the Finite Element Analysis Program (FEAP), developed by Taylor (2000). The elements developed for the nonlinear finite element analyses of RC bridge columns are a RC plane stress element and an interface element. Accompanying the present study, we attempted to implement a modified plane stress element and a modified RC shell element for the advanced hollow RC bridge column sections.

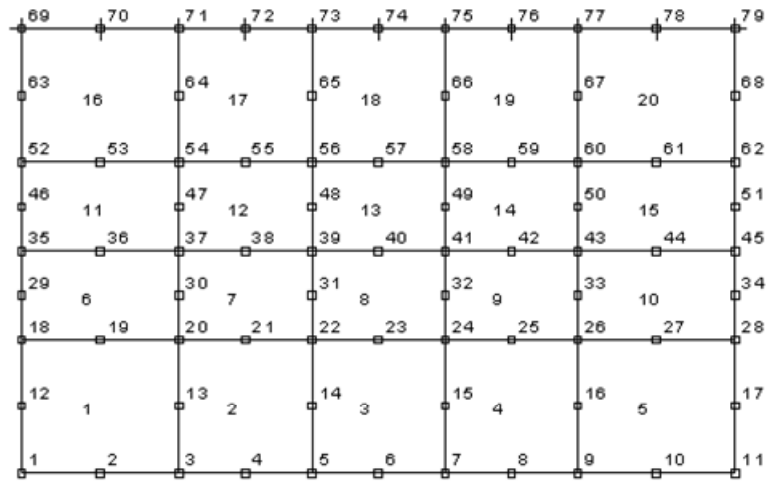
2D or 3D Spring element	4 nodes PSC shell element	2D or 3D Flexibility- based fiber beam-column element	4 nodes Elastic shell element
Joint element	FEAP		4 nodes RC shell element
Reinforcing or Prestressing bar element	Interface element	RC plane stress element	2D Elasto-plastic plane stress element

Fig. 12 RCAHEST nonlinear finite element analysis program

The nonlinear material model for the RC comprises models for concrete and models for the reinforcing bars. Models for concrete may be divided into models for uncracked concrete and for cracked concrete. For cracked concrete, three models describe the behavior of concrete in the direction normal to the crack plane, in the direction of the crack plane, and in the shear direction at the crack plane, respectively. The basic and widely-known model adopted for crack representation is based on the non-orthogonal fixed-crack method of the smeared crack concept. The post-yield constitutive law for the reinforcing bar in concrete considers the bond characteristics, and the model is a bilinear model.

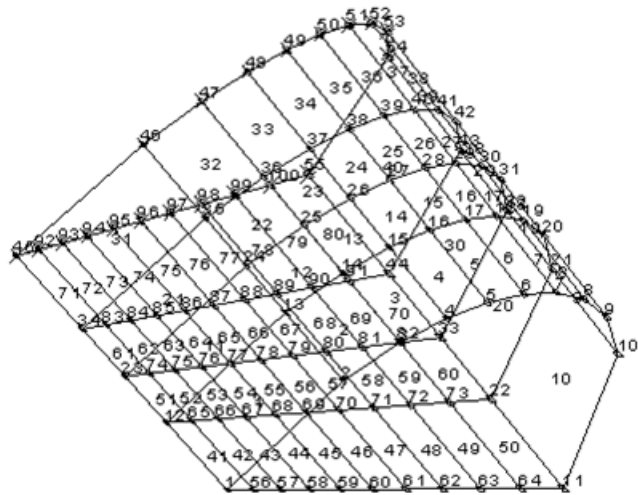
In this study, we adopted a lateral confining effect model, and incorporated it into the structural element library for RCAHEST, so that it can be used to assess the performance of advanced hollow RC bridge column sections with triangular reinforcement details. This is similar to the formula suggested by Mander *et al.* (1988) for the triaxial stress condition Shirmohammadi and Esmaeily (2015), but the reduced confinement effectiveness coefficient corresponding to the ratio

8-node RC plane stress element	20
---	-----------



(a)

4-node RC shell element	80
------------------------------------	-----------



(b)

Fig. 13 Finite element mesh for specimens: (a) rectangular sections; and (b) circular sections

of the inside-to-outside diameters of the bridge column section is applied. We have given details of the nonlinear material model used in previous research Kim *et al.* (2002, 2003, 2007, 2009, 2013, 2014).

We describe the modeling techniques of the advanced hollow RC bridge column sections with triangular reinforcement details in the following sections.

Fig. 13 shows the finite element discretization and the boundary conditions for rectangular specimens and circular specimens. The analytical portions of this study focused on the quasi-static, monotonic loading of hollow cross sections. We conducted the analysis in multiple steps to simulate the actual behavior of the specimen. We applied loading cycles with load control.

4.2 Comparison with experimental results

Fig. 14 compares the simulated and experimental axial load-axial strain values for a sample of specimens. The sample of specimens is the advanced hollow RC bridge column sections with triangular reinforcement details. The predicted strength was lower than the actual strength. The stiffness in the simulation is considerably greater than that of the experiment. In light of this, while considering the uncertainty in the boundary condition, and the fact that the hollow column sections had previously been tested, we can state that the analytical prediction concurs well with the experimental behavior.

The values given by all specimens were similar to the analytical results; Table 3 summarizes comparative data. In predicting the results of the specimens, the mean ratios of experimental-to-analytical maximum strength were 1.08 at a COV of 8%. The predictions of the failure modes of all the specimens also agree with the experimental results.

The proposed confinement model predicts quite well the behavior of hollow section confinement, in particular the strength increment and the remarkable ductility enhancement. The proposed model predictions usually slightly underestimate the experimental outcomes with a scatter of the order of less than ten percent.

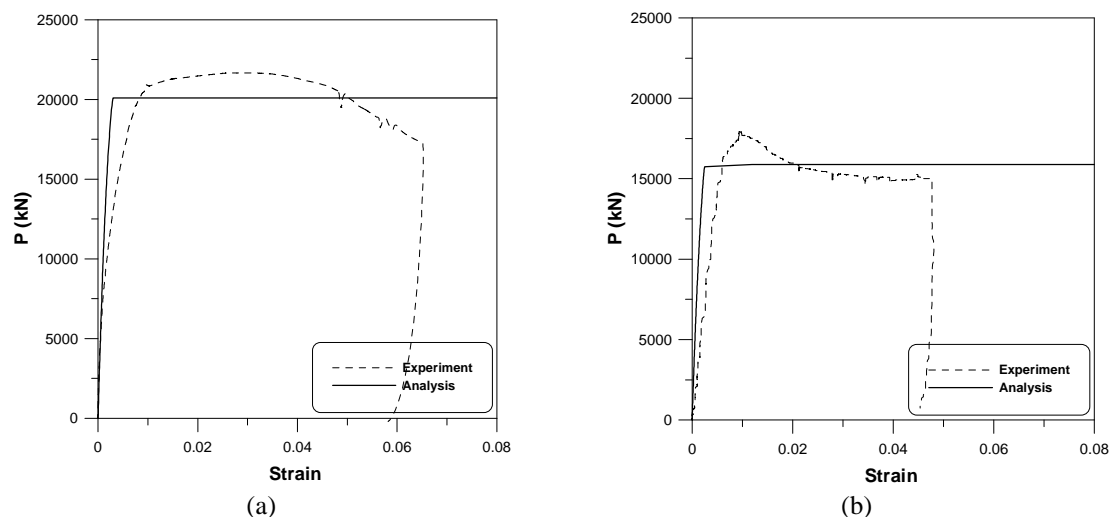


Fig. 14 Sample of comparison of results from the experimental results: (a) specimen C-RHT-BS; and (b) specimen C-CHT-IT

Table 3 Experimental and analytic results

Specimen	$P_{\max, \exp}$ (kN)	$P_{\max, \exp}$ (kN)	$P_{\max, \exp} / P_{\max, \text{ana}}$
C-RHC-BS	20475.3	20348.8	1.01
C-RHT-BS	21668.7	20103.7	1.08
C-RHT-IT	21647.5	19613.1	1.10
C-RHT-BD	21004.1	19123.0	1.10
C-RHT-BN	19512.4	18877.8	1.03
C-CHC-BS	14946.0	16319.2	0.92
C-CHT-BS	17638.8	16419.6	1.07
C-CHT-IT	17930.2	15884.7	1.13
C-CHT-BD	16303.7	14784.9	1.10
C-CHT-BN	18223.6	14733.2	1.24
Mean			1.08
Coefficient of variation			0.08

Nevertheless, numerical outcomes clearly show that to predict hollow column behavior, it is crucial to consider concrete cover spalling and steel reinforcement buckling. We consider the effect of concrete cover spalling and buckling of bars, key aspects of the proposed refined methodology, in the nonlinear analyses. These two brittle mechanisms acting together have a significant effect on the load carrying capacity and ductility of hollow column members.

Many parameters may influence the overall hollow column section response such as: the reinforcement details, the shape of the section, and the spacing of transverse reinforcement.

The experimental and analytical results and the parametric studies confirmed that for such hollow column sections with the innovative reinforcement details, the position of the neutral axis at failure with respect to the inside face of the section controls the available strength and ductility.

The importance of identifying and evaluating the adequacy of simulation methods is an important and necessary step in applying performance-based assessment techniques for assessing new, enhanced performance systems. Such assessment can help to speed the implementation of such systems in current applications.

5. Conclusions

This study investigated the performance of advanced hollow RC bridge column sections with triangular reinforcement details. We designed the proposed innovative reinforcement details under investigation in this study with the aim of achieving a degree of strength and ductility. We developed an analytical model that predicts the behavior of advanced hollow RC bridge column sections, with reinforcement details for material quantity reduction, that are subjected to simultaneous axial load.

From the results of the experimental and analytical studies, we reached the following conclusions.

1. We concluded an experimental and analytical study to quantify performance measures and examine one aspect of detailing for a set of developed innovative reinforcement details. We

concluded that the design concepts and construction methods are promising solutions to the application of advanced hollow RC bridge column sections with reinforcement details for material quantity reduction.

2. We found that all ten analyses predicted the experimental failure loads fairly well. We performed a finite element solution, incorporating material nonlinearities, and obtained satisfactory comparisons with the experimental results. These include both general criteria for the methods of analysis, and specific recommendations for the detailing of reinforcement.

3. The concurrence between the analytical and experimental axial load-axial strain relationship was generally sound. The mean ratio and coefficient of variation (COV) of experimental-to-analytical ultimate strength for specimens were 1.08 and 8%, respectively. We modified a confinement model for hollow sections. The model is able to estimate confinement effectiveness, which differs in the case of solid and hollow sections. Such an assessment tool can help to speed the implementation of advanced hollow column section systems in current applications.

4. Regarding the implementation of full-scale structures, we will in the future carry out an investigation of alternative construction details, performance under cyclic rather than quasi-static monotonic loading, and the development of design procedures and guidelines.

References

- AASHTO (2012), AASHTO LRFD "Bridge Design Specifications", 6th Edition.
- Delgado, P., Vila-Pouca, N., Arede, A., Rocha, P., Costa, A. and Delgado, R. (2008), "Experimental cyclic behavior of hollow-section bridge piers with different transverse reinforcement details", *Proceedings of the 14th World Conference on Earthquake Engineering*, Beijing, China.
- Eurocode 2 (2004), Design of Concrete Structures-Part 1: General Rules and Rules for Buildings, EN1992-1, European Committee for Standardization, Brussel.
- Han, Q., Zhou, Y., Dum, X., Huang, C. and Lee, G.C. (2014), "Experimental and numerical studies on seismic performance of hollow RC bridge columns", *Earthq. Struct.*, **7**(3) 251-269.
- Hoshikuma, J. and Priestley, M.J.N. (2000), "Flexural behavior of circular hollow columns with a single layer of reinforcement under seismic loading", Report No. SSRP-2000/13, University of California, San Diego, California.
- Kim, T.H. (2014), "Structural performance assessment of deteriorated reinforced concrete bridge piers", *Comput. Concrete*, **14**(4), 387-403.
- Kim, T.H., Choi, J.H., Lee, J.H. and Shin, H.M. (2013), "Performance assessment of hollow RC bridge column sections with reinforcement details for material quantity reduction", *Mag. Concrete Res.*, **65**(21), 1277-1292.
- Kim, T.H., Hong, H.K., Chung, Y.S. and Shin, H.M. (2009), "Seismic performance assessment of reinforced concrete bridge piers with lap splices using shaking table tests", *Mag. Concrete Res.*, **61**(9), 705-719.
- Kim, T.H., Kim, Y.J., Kang, H.T. and Shin, H.M. (2007), "Performance assessment of reinforced concrete bridge columns using a damage index", *Can. J. Civil Eng.*, **34**(7), 843-855.
- Kim, T.H., Lee, K.M. and Shin, H.M. (2002), "Nonlinear analysis of reinforced concrete shells using layered elements with drilling degree of freedom", *ACI Struct. J.*, **99**(4), 418-426.
- Kim, T.H., Lee, K.M., Yoon, C.Y. and Shin, H.M. (2003), "Inelastic behavior and ductility capacity of reinforced concrete bridge piers under earthquake. I: theory and formulation", *J. Struct. Eng.*, ASCE, **129**(9), 1199-1207.
- Lignola, G.P. (2006), "RC hollow members confined with FRP: experimental behavior and numerical Modeling", Ph.D. Thesis, University of Naples, Italy.
- Mander, J.B., Priestley, M.J.N. and Park, R. (1988), "Theoretical stress-strain model for confined concrete", *J. Struct. Eng.*, ASCE, **114**(8), 1804-1826.

- Ministry of Construction and Transportation (2010), Korea Highway Bridge Design Code.
- Papanikolaou, V.K. and Kappos, A.J. (2009), "Numerical study of confinement effectiveness in solid and hollow reinforced concrete bridge piers: methodology", *Comput. Struct.*, **87**(21-22), 1427-1439.
- Shirmohammadi, F. and Esmaily A. (2015), "Performance of reinforced concrete columns under bi-axial lateral force/displacement and axial load", *Eng. Struct.*, **99**, 63-77.
- Taylor, R.L. (2000), FEAP-A Finite Element Analysis Program, Version 7.2 Users Manual, 1 and 2.
- Yeh, Y.K., Mo, Y.L. and Yang, C.Y. (2002), "Seismic performance of rectangular hollow bridge columns", *J. Struct. Eng., ASCE*, **128**(1), 60-68.
- Yukawa, Y., Ogata, T., Suda, K. and Saito, H. (1999), "Seismic performance of reinforced concrete high pier with hollow section", *P. JPN Society Civil Eng.*, **42**(613), 103-120. (in Japanese)
- Zahn, F.A., Park, R. and Priestley, M.J.N. (1990), "Flexural strength and ductility of circular hollow reinforced concrete columns without confinement on inside face", *ACI Struct. J.*, **87**(2), 156-166.